Heliyon 9 (2023) e13315

Contents lists available at ScienceDirect

Heliyon

journal homepage: www.cell.com/heliyon

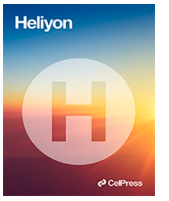

Research article

Extracellular vesicles from hypoxia-pretreated adipose-derived stem cells regulate hypoxia/reoxygenation-induced human dermal microvascular endothelial apoptosis and autophagy in vitro

M.M. Yinhua Zhao [a], M.M. Yanyu Shi [a,b], Huang Lin [a,*]

[a] Plastic and Reconstructive Surgery, Beijing Anzhen Hospital, Capital Medical University, Chaoyang District, Beijing, 100029, China
[b] Plastic and Reconstructive Surgery, Beijing Luhe Hospital, Capital Medical University, Tongzhou District, Beijing, 101149, China

ARTICLE INFO

Keywords:
Extracellular vesicles
Hypoxia/reoxygenation
Hypoxia-pretreated
Adipose-derived stem cells
Apoptosis and autophagy
Human dermal microvascular endothelial cells

ABSTRACT

Recent studies suggest hypoxia can promote adipose-derived stem cells (ADSCs) to attenuate hypoxia/reoxygenation (H/R)-induced damage to human dermal microvascular endothelial cells (HDMECs). Extracellular vesicles (EVs), isolated from ADSCs, play an-important role in the fields of regenerative medicine. Here, we aimed to investigate the effect of EVs isolated from hypoxia-pretreated ADSCs (ADSC-EVs[H]) on HDMECs to attenuate ischemia/reperfusion injury of free skin flaps. First, we characterized EVs isolated from normoxia-cultured ADSCs (ADSC-EVs[N]) and ADSC-EVs(H). Experimental data indicated that EVs isolated from ADSCs consisted of lipid-bilayer vesicles that exhibited positive expression of vascular endothelial growth factor (VEGF) and marker proteins CD9, CD63 and CD81, and the mean particle size of EVs in the hypoxia-pretreated ADSCs (ADSC[H]) group was smaller (74.17 nm) than in the normoxic-cultured ADSCs (ADSC[N]) group (93.87 nm). Hypoxic pretreatment increased the number of EVs. Later, we favorably constructed the co-culture model of EVs isolated from ADSCs (ADSC-EVs) and H/R-induced HDMECs. Cell counting kit-8, Ethynyldeoxyuridine assay, western blotting and immunofluorescence staining showed that ADSC-EVs(H) promoted the survival of HDMECs and increased LC3 level. Apoptosis, reactive oxygen species (ROS) and JC-1 mitochondrial membrane potential (MMP) assays revealed that ADSC-EVs(H) reduced the apoptosis rate and ROS accumulation and increased MMP level in HDMECs, indicating that ADSC-EVs(H) effectively attenuated H/R-induced damage in HDMECs through autophagy activation and the-inhibition of apoptosis and oxidative stress. This study confirmed that ADSC-EVs(H) could effectively regulate the proliferation, apoptosis, oxidative stress, and autophagy expression of H/R-induced HDMECs in vitro, and therefore the transplantation of ADSC-EVs(H) may provide novel insights for the transplantation of free skin flaps.

1. Introduction

Free skin flap transplantation is an important method to repair soft tissue defects in plastic and reconstructive medicine. However, ischemia/reperfusion (I/R) injury has limited the clinical application of free skin flaps [1].

Recent years, cell-based therapy with adipose-derived stem cells (ADSCs) has emerged as a promising tool in regenerative medicine

* Corresponding author.
E-mail address: linhuang_72@163.com (H. Lin).

https://doi.org/10.1016/j.heliyon.2023.e13315
Received 5 September 2022; Received in revised form 22 January 2023; Accepted 26 January 2023
Available online 29 January 2023
2405-8440/© 2023 The Authors. Published by Elsevier Ltd. This is an open access article under the CC BY-NC-ND license (http://creativecommons.org/licenses/by-nc-nd/4.0/).

[2]. As an important source of mesenchymal stem cells (MSCs), ADSCs play an important role in a variety of cellular functions, including promoting the survival of adipose grafts and angiogenesis, and alleviating reperfusion injury in the brain [3–5]. However, the mechanism remains controversial. One view is that MSCs could repair damage mainly by differentiating into target cells [6]; however, it has been shown that most MSCs died within 2 weeks after transplantation; and the remaining viable MSCs were insufficient to repair the damage [7]. Another hypothesis is that MSCs regulate cell damage mainly through paracrine factor [8].

As an important paracrine mediator between MSCs and target cells, extracellular vesicles (EVs) are involved in various pathological and physiological processes, including intercellular substance exchange and signal transduction [9]. For example, EVs can enhance angiogenesis [10]; and alleviate inflammation by carrying multiple components, including soluble proteins, mRNA and microRNA, into target cells [11–13]. Additionally, EVs from ADSCs (ADSC-EVs) can protect rat skin flaps, brain, and adipose tissues [3–5] against I/R injury.

Our previous study has demonstrated hypoxia promotes ADSCs to attenuate hypoxia/reoxygenation (H/R)-induced injury in human dermal microvascular endothelial cells (HDMECs). However, it remains unclear whether hypoxia-pretreated ADSC-EVs (ADSC-EVs[H]) can inhibit H/R-induced HDMECs injury. In this study, we aimed to 1) isolate and compare EVs isolated from normoxia-cultured ADSCs (ADSC-EVs[N]) and ADSC-EVs(H); and 2) investigate the effect of ADSC-EVs(H) on H/R-induced HDMECs injury and explore possible mechanisms.

2. Material and methods

2.1. Cell culture and EVs isolation

HDMECs and ADSCs were purchased from American Type Culture Collection (Washington, America). HDMECs were cultured as previous described [14]. ADSCs were cultured in Dulbecco's modified Eagle's medium (DMEM, Gibco, Grand island, America) containing 10% fetal bovine serum (FBS) and 1% penicillin/streptomycin solution [2].

EVs were extracted from the supernatants of ADSCs cultures using an Exosome Isolation kit (293–77601, Wako Pure Chemical Industries, Tokyo, Japan), following the manufacturer's instructions. Briefly, ADSCs were either transferred to DMEM containing 10% EV-depleted FBS and cultured in a normoxic incubator (95% air, 5% CO_2), or transferred to serum-free DMEM and cultured in a hypoxic incubator (93% N_2, 5% CO_2, 2% O_2). After 48 h, the medium was centrifuged at a rate of 1000 r/min for 10 min and the supernatant was filtered through 0.22 μm filters to remove dead cells and debris. The high purity EVs were extracted using Exosome Isolation kit. Magnetic beads made of Tim 4 protein were used to bind phosphatidyl serine (PS) on the surface of EVs in the presence of metal ions, then neutral elution buffer containing EDTA was used to elute the EVs. Isolation of EVs with high purity and integrity was achieved by the PS affinity method [15]. EVs were immediately used for experiments or stored at −80 °C. The experiments were approved by the Ethics Committee of Beijing Anzhen Hospital, Capital Medical University, China.

2.2. EVs assay

The proteins of EVs were detected using a bicinchoninic acid (BCA) protein assay kit (Thermo Fisher Scientific, Waltham, Massachusetts, America) according to the manufacturer's instructions. The optical density (OD) of proteins was measured at 562 nm by a microplate reader (Multiskan GO, Thermo Fisher Scientific). Marker proteins and vascular endothelial growth factor (VEGF) in EVs were detected using western blotting with the following antibodies: CD9 antibody (bs-2489 R, Bioss, Beijing, China), CD81 antibody (GTX31381, GeneTex, Southern California, America), VEGF antibody (AF5131, Affinity, Jiangsu, China), CD63 antibody (GTX41877, GeneTex) and β-actin (1:50,000; cat. No. AC026; ABclonal, China). The secondary antibody was a rabbit polyclonal secondary antibody to mouse IgG-H&L (ab6728, Abcam, Shanghai, China). The morphology of EVs was observed using a transmission electron microscope (JSM-IT300LV, JEOL, Beijing, China) with an EVs electron microscope analysis kit (Weihui Biology, Beijing, China). Finally, the diameter, distribution and number of EVs were analyzed by nanoparticle tracking analysis with a Nanosight NS300 (Beijing, China).

2.3. Experimental protocol

The HDMECs were randomly divided into four groups: 1) Control group, cultured under normoxic conditions (95% air, 5% CO_2); 2) H/R group, placed into a hypoxic incubator (94% N_2, 5% CO_2, 1% O_2) for 8 h then incubated under normal conditions for 24 h [14]; 3) H/R + ADSC-EVs(N) group, H/R group treatment followed by the addition of 20 μg ADSC-EVs(N) to the culture medium; and 4) H/R + ADSC-EVs(H) group, H/R group treatment followed by the addition of 20 μg ADSC-EVs(H) to the culture medium.

2.4. Cell proliferation

Cell Counting Kit-8 (CCK8, C0038, Beyotime, Shanghai, China) assay was used to determine the proliferation rate of HDMECs at 24 h, 48 h and 72 h, following the manufacturer's instructions. Briefly, cells were seeded into 96-well plates, 10 μL CCK8 solution was added to each well and incubated for 4 h at 37 °C. The OD at 450 nm was measured by a microplate reader.

According to the manufacturer's instructions, the Ethynyldeoxyuridine (EdU) Cell Proliferation Kit with Alexa Fluor 555 (cat. No. CX003, Cellor Lab, China) was used to conduct the EdU assay. Cells were cultured in 24-well dishes at a density of 1×10^4 cells per well. After 24 h of co-culture with ADSC-EVs, the cell medium was removed, and EdU-labeled (also called EdU+) medium was added to

24-well dishes and incubated at 37 °C for 2 h. Cells were first fixed with 4% paraformaldehyde for 15 min at room temperature and washed with PBS three times for 5 min, then permeabilized with 0.3% Triton X-100 at room temperature and washed with PBS three times for 5 min. Following that, 200 μL of click working solution was added to each well and incubated for 30 min under light-shading conditions. After washing three times with PBS, the nuclei were counterstained with Hoechest 33,342 for 10 min at room temperature. Finally, EdU + cells were observed using a fluorescence microscope (Nikon DS-Ri2, China) and shown as orange fluorescence. And Image processing and analysis was performed using Image J (version 1.51).

2.5. Apoptosis assay

Flow cytometry (FACSCalibur, BD Biosciences, Franklin Lakes, New Jersey, America) was used to assess the apoptosis rate of HDMECs co-cultured with ADSC-EVs for 24 h. To detect apoptotic cells, a fluorescein isothiocyanate (FITC) Annexin V (AV) Apoptosis Detection Kit I (556,547, BD Biosciences) was used according to manufacturer's instructions, under which AV labels apoptotic cells and propidium iodide (PI) marks necrotic cells.

2.6. Reactive oxygen species (ROS) assay

After co-cultured with ADSC-EVs for 24 h, the ROS level in HDMECs was measured using the ROS Assay Kit (S0033, Beyotime) according to the manufacturer's instructions. The light emission of cell samples was measured at a wavelength of 520 nm using a flow cytometer. ROS-positive cells showed strong green fluorescence.

2.7. JC-1 mitochondrial membrane potential (MMP)assay

Preparation of the JC-1 staining solution (Component A) and positive control were undertaken using a MMP kit (C2006-1, Beyotime) according to the manufacturer's instructions. After co-cultured with ADSC-EVs for 24 h, HDMECs were harvested and resuspended with 0.5 mL phosphate-buffered saline. Next, 0.5 mL JC-1 staining solution was added to each sample and incubated for 30 min at 37 °C. Cells were washed and resuspended twice with JC-1 buffer for analysis by flow cytometry.

2.8. Immunofluorescence staining

Immunofluorescence staining was used to detect the expression of microtubule-associated protein 1 A/1 B-light chain 3 (LC3) in HDMECs. Briefly, HDMECs were seeded on a 15-mm glass diameter (cat. No. 801007, Nest, Wuxi, China), which was then placed on a 24-well cell culture plate (cat. No. CCP-12H, Servicebio, China). After being co-cultured with ADSC-EVs for 24 h, cells were washed with PBS three times. Then the cells were fixed with 4% paraformaldehyde for 15 min and washed with PBS three times for 5 min. Then, HDMECs were permeabilized with 0.1% Triton X-100 (Sigma-Aldrich, Shanghai, Beijing) for 15 min and washed with PBS three times for 5 min. Blocked cells with 1% bovine serum albumin for 1 h at room temperature, then incubated with LC3 antibody (ab48394, Abcam, 1:100) at 4 °C for 12 h. After incubation with donkey anti-rabbit IgG H&L (ab6802, Abcam, 1:200) for 1 h at 37 °C in the dark, 4′,6-diamidino-2-phenylindole was used to stain the nuclei for 10 min. The images were captured under a fluorescence microscope (Olympus Corporation, Tokyo, Japan).

2.9. Western blotting

HDMECs were washed twice with cold PBS and exposed to RIPA lysis buffer containing a protease inhibitor for 20 min, followed by centrifugation at 15,000×*g* for 10 min at 4 °C. The protein concentration was determined using BCA method, and protein content was adjusted to achieve equal concentration and volumes. Next, protein samples were analyzed by 12.5% sodium dodecyl sulfate (SDS)-polyacrylamide gel electrophoresis and transferred onto a polyvinylidene fluoride membrane. Samples were then incubated with primary antibodies at 4 °C for 12 h, including LC3 (1:1000; cat. No. A17424; ABclonal, China) and β-actin (1:50,000; cat. No. AC026; ABclonal, China). Secondary antibody incubation was then performed using IRDye 680 Goat anti-Rabbit IgG (H + L) (1:10,000, cat. No. C80605-15; LiCOR, America) and Donkey anti-mouse IgG (H + L) (1:10,000, cat. No. Ab175738; Abcam, Shanghai). Protein bands were visualized and quantified using an Odyssey Infrared Imaging system (Gene Company, Ltd., Beijing, China).

2.10. Statistical analysis

All statistical analyses were performed with SPSS 20.0 version (IBM, State of California, America). Differences among groups were analyzed by one-way analysis of variance and two-factor analysis of variance. The normality of the data distribution was confirmed using the Shapiro–Wilk test, while the homogeneity of variance was confirmed using the F-test. Pairwise comparisons within groups were conducted using the Student–Newman–Keuls q test. For all comparisons, $P < 0.05$ was considered statistically significant. All data are presented as mean ± standard deviation.

3. Results

3.1. Characteristic changes in ADSC-EVs after hypoxic pretreatment

The concentration of EV proteins extracted from ADSCs cultured under normoxic conditions (0.1899 ± 0.0130 mg/mL) was significantly increased after hypoxic pretreatment (0.3022 ± 0.0139 mg/mL; $P < 0.01$; Fig. 1A). The marker proteins CD9, CD63, and CD81, as well as VEGF in EVs, were expressed in both normoxic-cultured ADSCs (ADSC[N]) and hypoxia-pretreated ADSCs (ADSC[H]) groups (Fig. 1B). Furthermore, the EVs, extracted from the ADSC(H) groups were retained characteristic cup-shaped morphology (Fig. 1C and D). The results of the nanoparticle tracking analysis revealed that the majority of EVs were between 30 and 160 nm in diameter (Fig. 1E), with the mean particle size of EVs in the ADSC(H) group (74.17 nm) being less than that of the ADSC(N) group (93.87 nm) (Fig. 1F) ($P < 0.05$). Conversely, hypoxic pretreatment induced more EVs production in ADSCs, and the concentration of EVs increased from 1.03×10^8/mL in the ADSC(N) group to 4.52×10^8/mL in the ADSC(H) group ($P < 0.05$, Fig. 1G). Taken together, the results of present study demonstrated that the character of EVs were changed after hypoxic pretreatment.

3.2. ADSC-EVs(H) attenuated the inhibitory effect of H/R on HDMEC proliferation

The proliferation ability of HDMECs co-cultured with ADSC-EVs for 24 h, 48 h and 72 h were tested using the CCK8 assay. The OD value at 450 nm denoted the cell proliferation rate (Fig. 2A). At 24 h, the proliferation rate of HDMECs did not differ significantly

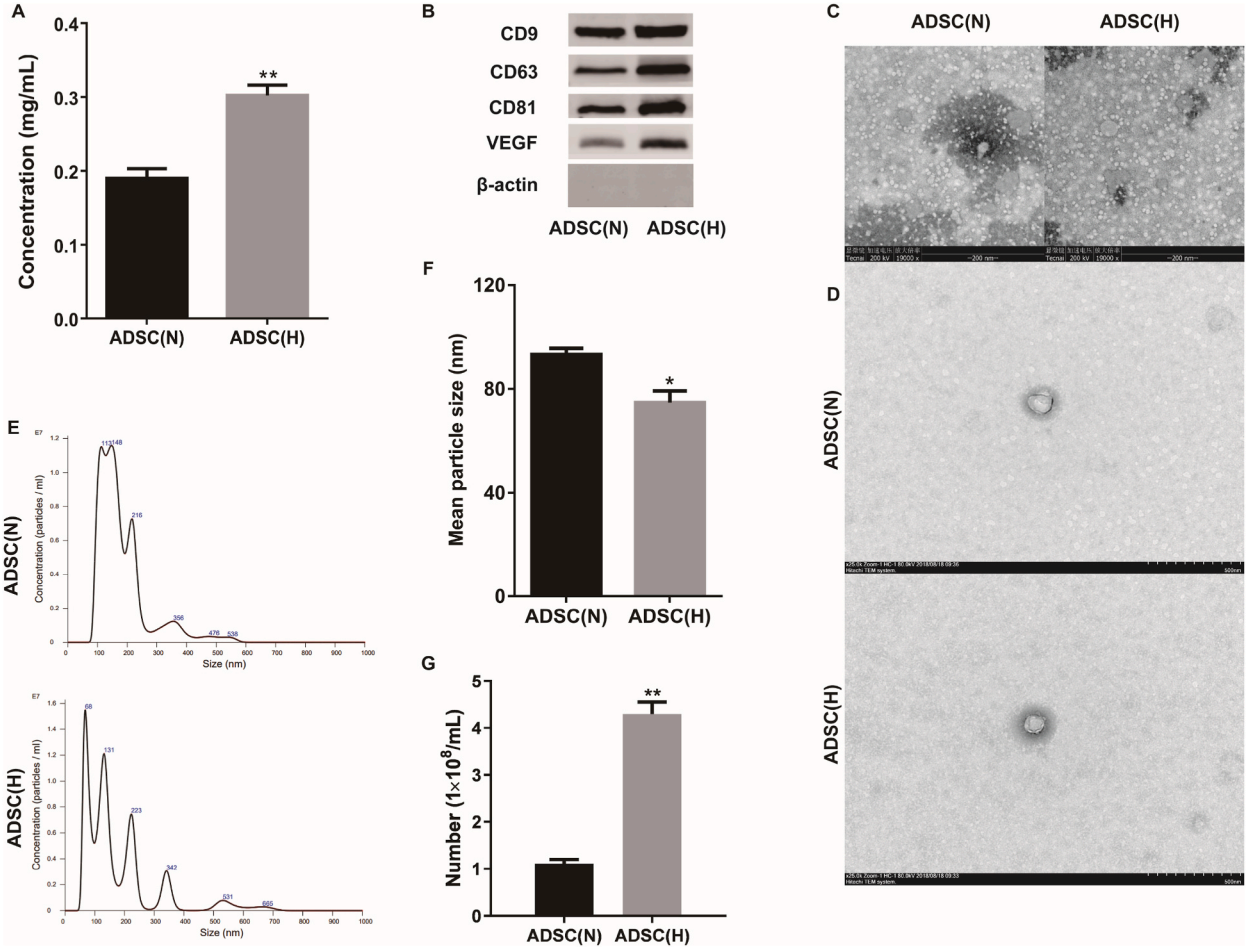

Fig. 1. Characteristic changes in the extracellular vesicles (EVs) of adipose-derived stem cells (ADSCs) after hypoxic pretreatment. (A) Protein concentrations in hypoxia-pretreated ADSCs (ADSC[H]) and normoxia-cultured ADSCs (ADSC[N]). (B) Western blotting of proteins. Expression of β-actin, vascular endothelial growth factor (VEGF) and EV-specific markers (CD9, CD63 and CD81) were used to verify the vesicle purity of the EVs. Transmission electron microscopy showed the morphology of EVs (scale bar = 200 nm, magnification = 19,000 ×) (C) and maintenance of the characteristic cup-shaped morphology in the ADSC(H) group (scale bar = 500 nm) (D). Nanoparticle tracking analysis of EVs in ADSC(H) and ADSC (N) showed the changes of particle size distribution (E); mean particle size (F); and number of per milliliter (G); *$P < 0.05$ vs. ADSC(N); **$P < 0.01$ vs. ADSC(N).

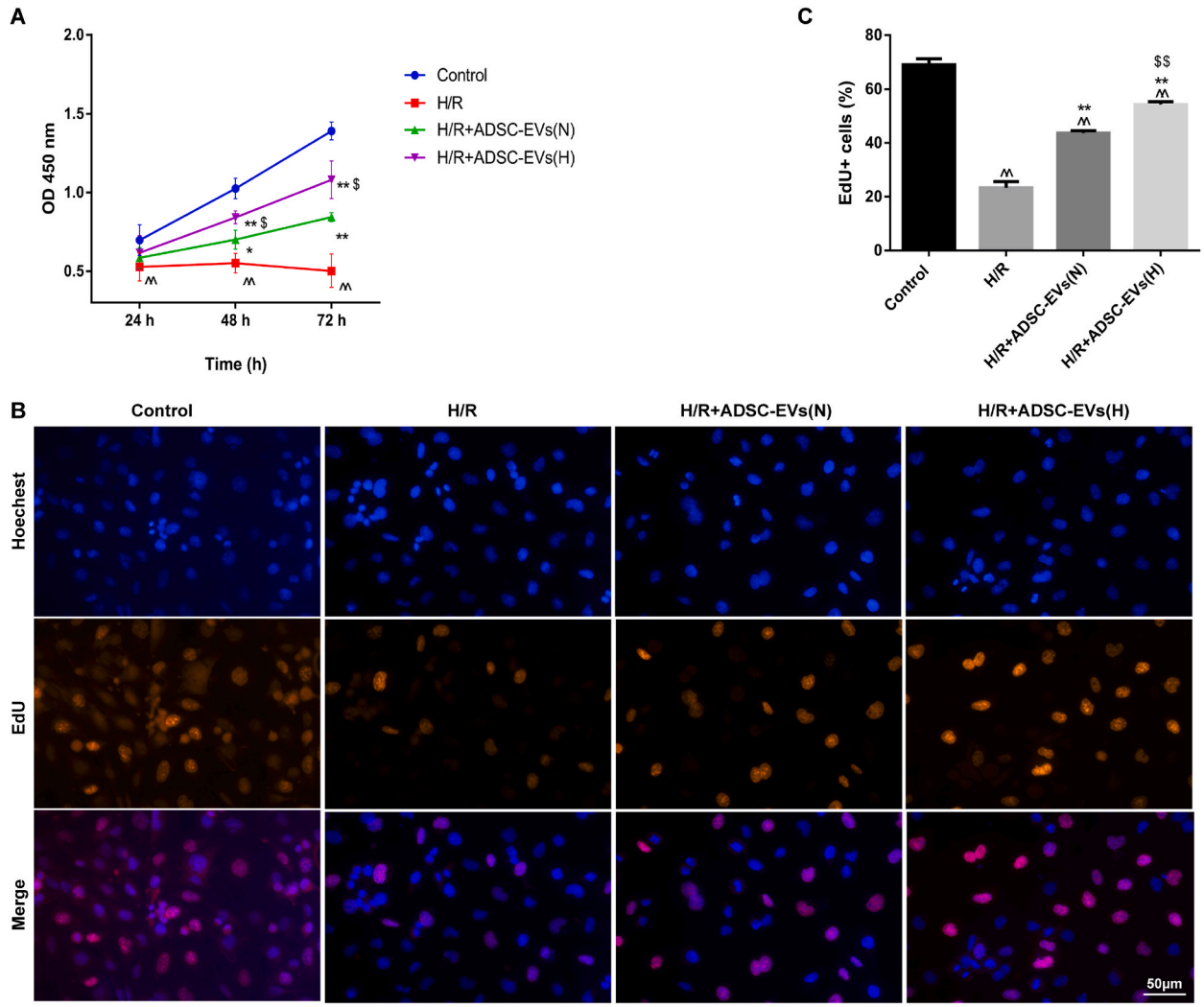

Fig. 2. Proliferation rates of human dermal microvascular endothelial cells (HDMECs) in the four groups. (A) Cell Counting Kit 8 was used to test the proliferation rate of HDMECs, and the results were expressed as the absorbance (optical density) at 450 nm. (B) The Ethynyldeoxyuridine (EdU) assay was used to detect the DNA replication ability of HDMECs. The EdU + cells were stained as orange. The nuclei were counterstained with Hoechst 33,342 (blue). The Merge panel showed the results of superimposed fluorescence. Magnification, × 400. Scale bar, 50 μm. (C) Comparison of EdU + cells in the four groups. HDMECs in Control group were cultured under normoxic conditions (95% air, 5% CO_2). For the hypoxia/reoxygenation (H/R) group, HDMECs were placed in a hypoxic incubator (94% N_2, 5% CO_2, 1% O_2) for 8 h, then incubated under normal conditions for 24 h. In the H/R + ADSC-EVs(N) and H/R + ADSC-EVs(H) groups, HDMECs underwent H/R treatment followed by the addition of 20 μg of EVs from normoxia-cultured adipose-derived stem cells (ADSC-EVs[N]) or hypoxia-pretreated ADSCs (ADSC-EVs[H]) to the culture medium respectively. $^{\wedge}P < 0.01$ vs. Control, $^{*}P < 0.05$ vs. H/R, $^{**}P < 0.01$ vs. H/R, $^{\$}P < 0.05$ vs. H/R + ADSC-EVs(N). (For interpretation of the references to colour in this figure legend, the reader is referred to the Web version of this article.)

between the Control, H/R, H/R + ADSC-EVs(N), and H/R + ADSC-EVs(H) groups, 0.71 ± 0.07, 0.53 ± 0.09, 0.59 ± 0.07, 0.63 ± 0.08, respectively ($P > 0.05$).

At 48 h, the cell proliferation rate in Control and H/R groups was significantly different at 0.97 ± 0.09 and 0.54 ± 0.05, respectively, ($P < 0.01$). Compared with the H/R group, the proliferation rates in H/R + ADSC-EVs(N) and H/R + ADSC-EVs(H) groups were significantly higher at 0.68 ± 0.07 ($P < 0.05$) and 0.84 ± 0.09 ($P < 0.01$), respectively. ADSC-EVs(H) significantly reduced the inhibitory effect of H/R on HDMEC proliferation.

At 72 h, the difference in cell proliferation between the Control (1.37 ± 0.01) and H/R group (0.50 ± 0.09) continued to increase ($P < 0.01$), indicating that H/R induced irreversible damage to HDMECs in the absence of intervention. Conversely, after co-cultured with ADSC-EVs, the proliferation rate was significantly increased in both H/R + ADSC-EVs(N) (0.80 ± 0.09) and H/R + ADSC-EVs(H) (1.10 ± 0.05) groups, and ADSC-EVs(H) had a stronger promotion on HDMEC proliferation ($P < 0.05$). In addition, the proliferation of HDMECs was gradually enhanced with the prolongation of co-culture time with ADSC-EVs(H).

The EdU assay was used to test the proliferation of HDMECs by detecting the replication activity of DNA (Fig. 2B and C). EdU + cells

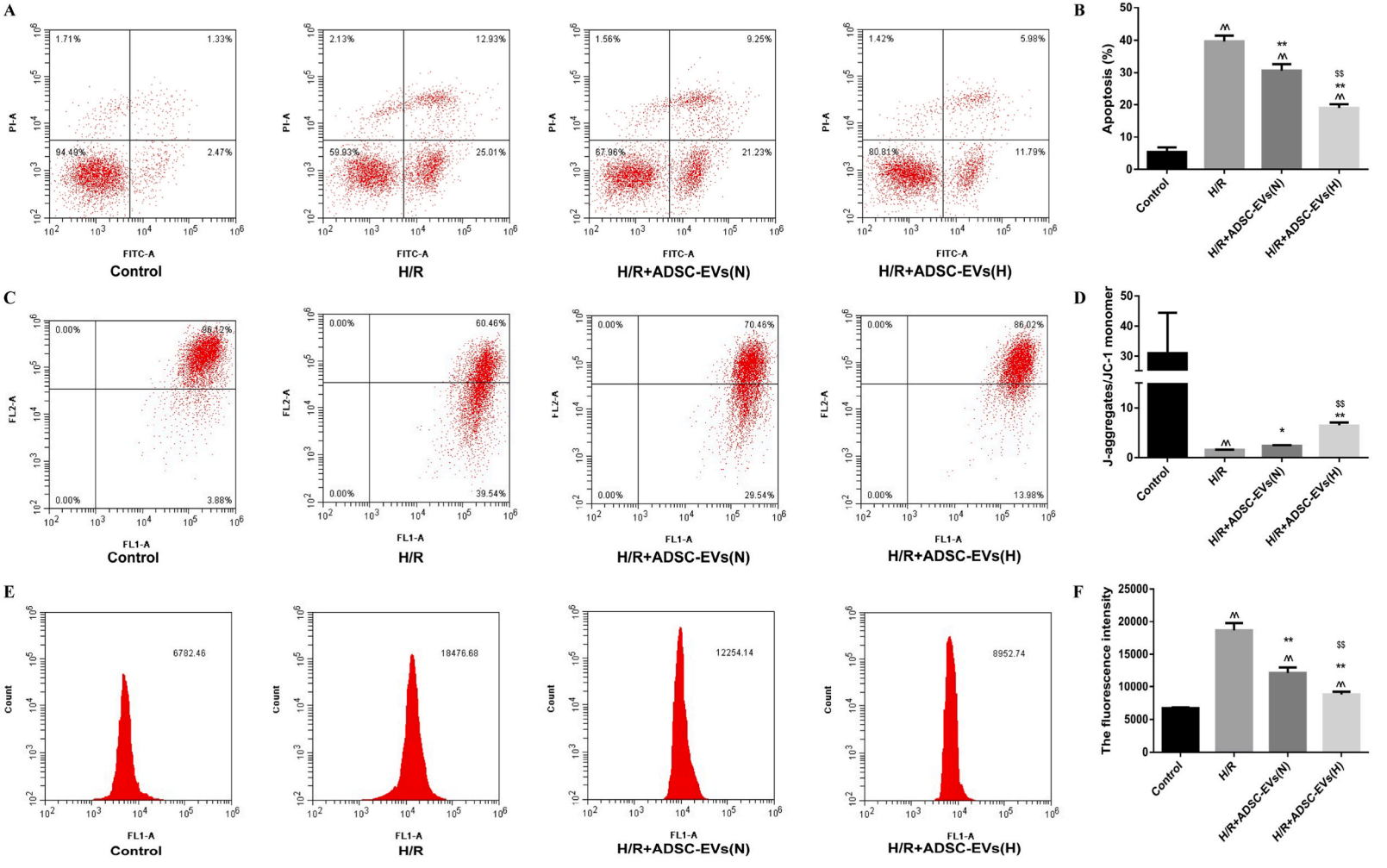

Fig. 3. Extracellular vesicles (EVs) from hypoxia-pretreated adipose-derived stem cells (ADSC-EVs[H]) reduced hypoxia/reoxygenation-induced cellular and mitochondrial apoptosis and reactive oxygen species (ROS) accumulation. (A) Scatter diagrams of flow cytometry results of the four groups: untreated Control human dermal microvascular endothelial cells (HDMECs); hypoxia/reoxygenation (H/R) treated HDMECs; H/R + ADSC-EVs(N) and H/R + ADSC-EVs(H), H/R treated HDMECs co-cultured with EVs from normoxia-cultured adipose-derived stem cells (ADSC-EVs[N]) or ADSC-EVs(H), respectively, for 24 h. Each dot plot shows the following: upper left quadrant, necrotic cells; upper right quadrant, late apoptotic cells positive for annexin-V fluorescein isothiocyanate (annexin-V FITC) and propidium iodide (PI); lower left quadrant, viable cells, which exclude annexin-V FITC and PI; and lower right quadrant, early apoptotic cells positive for annexin-V FITC and negative for PI. Apoptotic cells are represented by the percentage of annexin-V FITC single-positive and annexin-V FITC/PI double-positive cells. (B) Comparison of apoptosis rates among the four groups. (C) Scatter diagrams of cellular mitochondrial membrane potential expressed using percentage positivity of JC-1 dye in the FL1-A & FL2-A channels. (D) Comparison of J-aggregate/JC-1 monomer ratios, which represent the mitochondrial membrane potential, in each group. (E) Flow cytometry evaluation of ROS production in HDMECs. Strong green fluorescence of ROS-positive cells in the FL1-A channel. (F) Comparison of ROS production, as expressed by fluorescence intensity, in the four groups. Data expressed as mean ± standard deviation. $^{\wedge\wedge}P < 0.01$ vs. Control; $^{**}P < 0.01$ vs. H/R; $^{\$\$}P < 0.01$ vs. H/R + ADSC-EVs(N). FITC-A, annexin-V FITC. PI-A, PI. (For interpretation of the references to colour in this figure legend, the reader is referred to the Web version of this article.)

showed orange fluorescence and the nuclei were counterstained with Hoechst 33,342 and showed blue fluorescence. The EDU + cells rate indicated that the number of EdU + cells divided by the number of nuclei. After the H/R treatment, the EdU + cells rate (23.4 ± 2.3%) was significantly decreased compared with the Control group (69.1 ± 2.2%) ($P < 0.01$). However, the EdU + cells rate in the H/R + ADSC-EVs(N) group (43.7 ± 0.8%) was higher than that in the H/R group ($P < 0.01$). Importantly, the EdU + cells rate in the H/R + ADSC-EVs(H) group (54.3 ± 1.1%) was significantly higher than that in the H/R + ADSC-EVs(N) group ($P < 0.01$). Taken together, the results of present study demonstrated that ADSC-EVs(H) had better cytoprotective effect than ADSC-EVs(N) in promoting the proliferation of H/R-treated HDMECs.

3.3. ADSC-EVs(H) inhibited H/R-induced apoptosis in HDMECs and mitochondria

We investigated the apoptosis of H/R-induced HDMECs after co-cultured with ADSC-EVs for 24 h by flow cytometry (Fig. 3A and B). H/R significantly induced apoptosis in HDMECs (39.69 ± 1.74%, $P < 0.01$), compared with Control (5.36 ± 1.40%). However, the apoptosis rates in H/R + ADSC-EVs(N) and H/R + ADSC-EVs(H) groups were 30.69 ± 1.98% and 19.05 ± 1.15% ($P < 0.01$), demonstrating that ADSC-EVs(H) had a strong inhibitory effect on H/R-induced apoptosis in HDMECs.

The reduction of MMP is a landmark event in the early stage of apoptosis. The results were expressed by J-aggregate/JC-1 monomer ratio (Fig. 3C and D). Compared with Control (24.36 ± 2.30), the J-aggregate/JC-1 monomer ratio was significantly lower in the H/R group (1.54 ± 0.06) ($P < 0.05$), indicating that H/R induced additional JC-1 monomers production, leading to the depolarization of the mitochondrial membrane, and thus increasing the level of mitochondrial apoptosis. Compared with the H/R group, the J-aggregate/JC-1 monomer ratio was significantly higher after co-cultured with ADSC-EVs ($P < 0.05$), with 2.38 ± 0.12 for H/R + ADSC-EVs

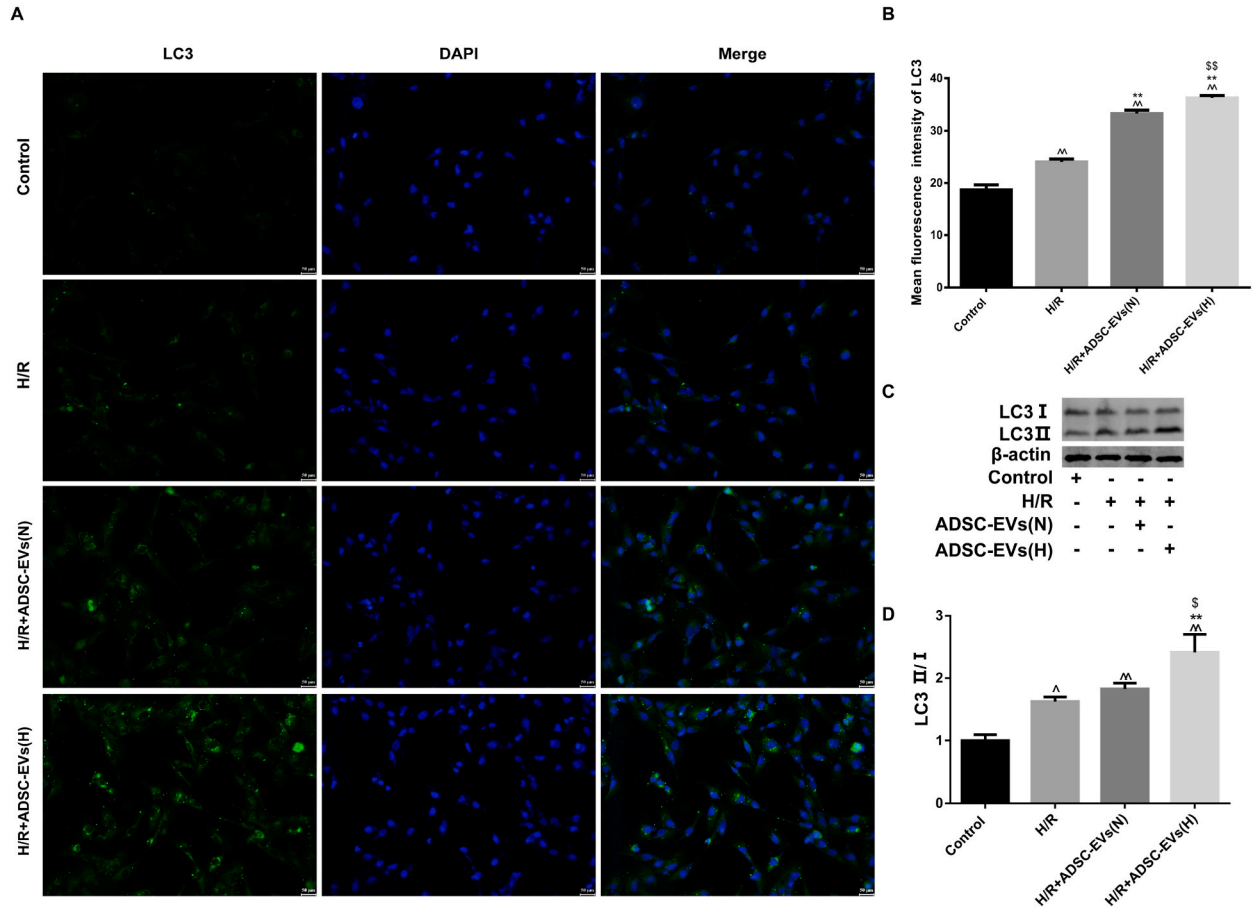

Fig. 4. Expression of microtubule-associated protein 1 A/1 B-light chain 3 (LC3) in human dermal microvascular endothelial cells (HDMECs) in the four groups. Untreated Control HDMECs; hypoxia/reoxygenation (H/R)-treated HDMECs; H/R + ADSC-EVs(N) and H/R + ADSC-EVs(H), H/R-treated HDMECs were co-cultured with EVs from normoxia-cultured adipose-derived stem cells (ADSC-EVs[N]) or hypoxia-pretreated ADSCs (ADSC-EVs[H]). (A) Immunofluorescence staining (green) of LC3, showing increased accumulation in the HR + ADSC-EVs(H) group. Nuclei stained with 4′,6-diamidino-2-phenylindole (DAPI) were blue. The Merge panel showed the results of superimposed fluorescence. Magnification, × 400. (B) Comparison of mean fluorescence intensity of LC3 immunofluorescent staining in the four groups; (C) Evaluation of the protein expression ratio of LC3 II/I (D) by western blotting analysis of the relative expression of LC3 II/I using β-actin as an internal control. ^^$P < 0.01$ vs. Control; **$P < 0.01$ vs. H/R; $^{\$\$}P < 0.01$ vs. H/R + ADSC-EVs(N).

(N) and 6.46 ± 0.67 for H/R + ADSC-EVs(H) ($P < 0.01$). The results revealed that ADSC-EVs significantly reduced H/R-induced mitochondrial membrane depolarization and apoptosis, particularly ADSC-EVs(H).

3.4. ADSC-EVs(H) reduced H/R-induced ROS accumulation in HDMECs

Flow cytometry results in Fig. 3E and F showed the ROS level of HDMECs in the four groups expressed as fluorescence intensity. Fluorescence intensity in the H/R group (18651.80 ± 1102.32) was significantly higher than in the Control group (6708.64 ± 138.06) ($P < 0.01$), indicating that H/R induced additional ROS production in HDMECs. With ADSC-EVs co-cultured for 24 h, the fluorescence intensity significantly decreased ($P < 0.01$). Furthermore, the fluorescence intensity was significantly lower in ADSC-EVs(H) group (8811.39 ± 405.38) compared with H/R + ADSC-EVs(N) group (12155.20 ± 842.14; $P < 0.01$). ADSC-EVs(H) strongly reduced H/R-induced ROS accumulation.

3.5. ADSC-EVs(H) promoted autophagy induction in HDMECs

The expression of LC3 was detected using immunofluorescence and western blotting after HDMECs were co-cultured with ADSC-EVs for 24 h (Fig. 4). Among the four groups of HDMECs, the fluorescence intensity of LC3 was lowest in the Control group ($P < 0.01$, Fig. 4A and B). Spots of LC3 fluorescence indicative of aggregation appeared in H/R group and were significantly enhanced after co-culture with ADSC-EVs for 24 h ($P < 0.01$), particularly in the ADSC-EVs(H) group ($P < 0.01$), indicating that hypoxic pretreatment enhance the autophagy induced by ADSC-EVs in HDMECs.

The ratio of LC3 II/I was tested to evaluate autophagy level of HDMECs (Fig. 4C and D). Compared with the Control, the ratio of LC3 II/I was significant increase in the H/R group ($P < 0.05$). Importantly, the ratio of LC3 II/I in the H/R + ADSC-EVs(H) group was evidently higher than that in the H/R group ($P < 0.01$), but not obviously in the H/R + ADSC-EVs(N) group ($P > 0.05$). Taken together, the results of present study indicated that hypoxia-pretreated ADSC-EVs activated the autophagy of HDMECs.

4. Discussion

In this study, we investigated the effect of hypoxic pretreatment on ADSC-EVs and the effect of the EVs on H/R-induced damage in HDMECs. Our results clearly demonstrated that hypoxic pretreatment promoted additional secretion of EVs by ADSCs, and that ADSC-EVs(H) enhanced proliferation and autophagy and inhibit H/R-induced apoptosis and ROS accumulation, more significantly than ADSC-EVs(N) in HDMECs. To our knowledge, this is the first study to report the protective effects of ADSC-EVs(H) on H/R-induced damage in HDMECs in vitro.

Currently, the protective mechanism of MSCs remains controversial. The advantages of using MSCs in flap transplantation involve differentiation and paracrine signaling. In a report using a mouse random flap model, only 20.81% of microvascular endothelial cells were differentiated from ADSCs [7]. Researchers also found that most MSCs died within 2 weeks after transplantation [16], indicating that differentiation alone is not sufficient to repair the lesions [7]. Therefore, paracrine signaling may be the main mechanism underlying the cytoprotective effect of MSCs. Gnecchi et al. reported that intramuscular injection of medium after culturing MSCs could reduce the area of myocardial infarction [17]. In this study, we successfully demonstrated that paracrine signaling was an important pathway for ADSC-mediated protection, and that ADSC-EVs are the true implementors of protection against H/R injury in HDMECs.

Moderate hypoxia can activate adaptive cellular responses, including secretion of survival and proangiogenic factors that match the supply of O_2 [18–20]. In this research, hypoxic pretreatment induced significantly more EVs to be released from ADSCs and increased the expression of VEGF in ADSC-EVs. Johnsen et al. found that knockdown of hypoxia-inducible factor 1 α (HIF-1α) resulted in a significant decrease in EVs in MSCs [20]. Zhang et al. reported that inhibition of HIF-1α inhibited VEGF expression in a time-dependent manner [21]. Therefore, we inferred that hypoxic pretreatment might enhance EVs secretion by activating the HIF-1α/VEGF signaling pathway. EVs functioning through paracrine or autocrine approaches might promote the adaptation of ADSCs to the hypoxic microenvironment.

ADSC-EVs(H) had the ability to promote the proliferation of HDMECs at the cellular level, with a significant time-to-effect relationship. However, statistical significance was not reached until 48 h. Yudi Han et al. reported that the proportion of EVs entering human umbilical vein endothelial cells was significantly higher after 12 h of co-culture than 6 h [22], indicating that, over time, more and more EVs entered endothelial cells to promote cell proliferation, and that angiogenic proteins encapsulated within the EVs directly promoted cell proliferation and triggered the transcription of angiogenic genes [23]. They also found that the proliferation of these cells peaked at 12 h of co-culture with ADSC-EVs and hypothesized that the effect of ADSC-EVs was temporary and lapsed after 12 h. Its protective effect was diminished after endocytosis and degradation of angiogenic proteins by target cells [22]. While ADSC-EVs were performed prior to hypoxia in HDMECs in this research. We speculated that different cellular processes might be responsible for the different phenomena, and the H/R treatment of HDMECs delayed the endocytosis, resulting in postponed effect of ADSC-EVs.

Weizhong Wang et al. reported that reperfusion injury is an important cause of free skin flap necrosis [24]. And the death of HDMECs is an important feature of reperfusion injury of free skin flap transplantation. At the reperfusion stage, high levels of ROS, endothelium-derived relaxing factor, and pro-inflammatory cytokines such as tumor necrosis factor α and interleukin-1 are released from ischemic tissues [25], resulting in leukocyte infiltration, interstitial edema, apoptosis and autophagy [26]. Reperfusion can also cause mitochondrial respiratory chain dysfunction by damaging complexes I, II and IV, resulting in mitochondrial membrane depolarization and mitochondrial outer membrane rupture, leading to the release of cytochrome C into the cytoplasm and activation of the autophagy and apoptosis pathway. To further investigate the mechanisms possibly responsible for the protective effect of ADSC-EVs

(H), we assessed the levels of ROS, MMP and apoptosis. The results demonstrated that ADSC-EVs(H) prior to hypoxia inhibited ROS accumulation, mitochondrial membrane depolarization and apoptosis rate; this indicated that the mitochondrial damage and apoptosis could be inhibited by ADSC-EVs(H).

The relationship between autophagy and apoptosis is complex. In most cases, autophagy is a physiologic process for tissue survival, whereas apoptosis removes the debris in the presence of tissue injury. Cytoprotective autophagy tends to be anti-apoptotic rather than pro-apoptotic and constitutes an initial barrier against apoptosis at low stress intensity. However, at high stress intensity, the induction of apoptosis results in the subversion of cytoprotective autophagy and the conversion of cytoprotective molecules into cytotoxic ones [27]. In that circumstance, cleavage of essential autophagy-related proteins not only inactivates the autophagic machinery but also leads to the generation of protein fragments with novel pro-apoptotic properties [27]. However, there are only several examples of autophagy having a promotion effect of apoptosis [28]. In this study, ADSC-EVs(H) attenuated the damage of HDMECs by activating autophagy and inhibiting apoptosis. The mechanism might be that the ADSC-EVs(H) would increase the threshold of stress required to induce apoptosis, thus HDMECs underwent cytoprotective autophagy rather than lethal apoptosis.

This study also has some limitations. First, the alterations in capacity of angiogenesis of HDMECs after H/R and EVs treatment were not investigated but is planned for a future study. Second, the mechanism of ADSC-EVs(H) in inhibiting apoptosis was not investigated but is planned for a future study. Third, the animal experiments were not performed to further elucidate the protective effect of hypoxia-pretreated ADSC-EVs on HDMECs.

Conclusions

Our study demonstrated that ADSC-EVs(H) effectively regulated H/R induced HDMECs proliferation, apoptosis, oxidative stress, and autophagy in vitro, and therefore the transplantation of ADSC-EVs(H) may provide new insights for free skin flaps transplantation.

Author contribution statement

Yinhua Zhao: Conceived and designed the experiments; Performed the experiments; Analyzed and interpreted the data; Contributed reagents, materials, analysis tools or data; Wrote the paper.

Yanyu Shi: Performed the experiments; Analyzed and interpreted the data; Wrote the paper.

Huang Lin: Conceived and designed the experiments; Contributed reagents, materials, analysis tools or data; Wrote the paper.

Funding statement

Mr. Huang Lin was supported by National Natural Science Foundation of China [81571922 and 81971849]; Natural Science Foundation of Beijing Municipality [7212026 and 7172065].

Data availability statement

Data will be made available on request.

Declaration of interest's statement

The authors declare that they have no known competing financial interests or personal relationships that could have appeared to influence the work reported in this paper.

Additional information

No additional information is available for this paper.

Appendix A. Supplementary data

Supplementary data to this article can be found online at https://doi.org/10.1016/j.heliyon.2023.e13315.

References

[1] K. Knight, Review of postoperative pharmacological infusions in ischemic skin flaps, Microsurgery 15 (1994) 675–684, https://doi.org/10.1002/micr.1920151004.

[2] Y. Zhao, Y. Shi, H. Lin, Hypoxia promotes adipose-derived stem cells to protect human dermal microvascular endothelial cells against hypoxia/reoxygenation injury, J. Surg. Res. 266 (2021) 230–235, https://doi.org/10.1016/j.jss.2021.04.013.

[3] C. Pu, C. Liu, C. Liang, et al., Adipose-derived stem cells protect skin flaps against ischemia/reperfusion injury via IL-6 expression, J. Invest. Dermatol. 137 (2017) 1353–1362, https://doi.org/10.1016/j.jid.2016.12.030.

[4] X. Huang, J. Ding, Y. Li, et al., Exosomes derived from PEDF modified adipose-derived mesenchymal stem cells ameliorate cerebral ischemia-reperfusion injury by regulation of autophagy and apoptosis, Exp. Cell Res. 371 (2018) 269–277, https://doi.org/10.1016/j.yexcr.2018.08.021.
[5] Y. Han, Y. Bai, X. Yan, et al., Co-transplantation of exosomes derived from hypoxia-preconditioned adipose mesenchymal stem cells promotes neovascularization and graft survival in fat grafting, Biochem. Biophys. Res. Commun. 497 (2018) 305–312, https://doi.org/10.1016/j.bbrc.2018.02.076.
[6] S. George, M. Hamblin, H. Abrahamse, Differentiation of mesenchymal stem cells to neuroglia: in the context of cell signalling, Stem cell reviews and reports 15 (2019) 814–826, https://doi.org/10.1007/s12015-019-09917-z.
[7] A. Uysal, H. Mizuno, M. Tobita, R. Ogawa, H. Hyakusoku, The effect of adipose-derived stem cells on ischemia-reperfusion injury: immunohistochemical and ultrastructural evaluation, Plast. Reconstr. Surg. 124 (2009) 804–815, https://doi.org/10.1097/PRS.0b013e3181b17bb4.
[8] M. Mirotsou, T. Jayawardena, J. Schmeckpeper, M. Gnecchi, V. Dzau, Paracrine mechanisms of stem cell reparative and regenerative actions in the heart, J. Mol. Cell. Cardiol. 50 (2011) 280–289, https://doi.org/10.1016/j.yjmcc.2010.08.005.
[9] M. Abdelgawad, N. Bakry, A. Farghali, A. Abdel-Latif, A. Lotfy, Mesenchymal stem cell-based therapy and exosomes in COVID-19: current trends and prospects, Stem Cell Res. Ther. 12 (2021) 469, https://doi.org/10.1186/s13287-021-02542-z.
[10] T. Ma, B. Fu, X. Yang, Y. Xiao, M. Pan, Adipose mesenchymal stem cell-derived exosomes promote cell proliferation, migration, and inhibit cell apoptosis via Wnt/β-catenin signaling in cutaneous wound healing, J. Cell. Biochem. 120 (2019) 10847–10854, https://doi.org/10.1002/jcb.28376.
[11] O. De Jong, B. Van Balkom, R. Schiffelers, C. Bouten, M. Verhaar, Extracellular vesicles: potential roles in regenerative medicine, Front. Immunol. 5 (2014) 608, https://doi.org/10.3389/fimmu.2014.00608.
[12] Z. Liu, Y. Xu, Y. Wan, J. Gao, Y. Chu, J. Li, Exosomes from adipose-derived mesenchymal stem cells prevent cardiomyocyte apoptosis induced by oxidative stress, Cell death discovery 5 (2019) 79, https://doi.org/10.1038/s41420-019-0159-5.
[13] R. Kalluri, V. LeBleu, The Biology Function and Biomedical Applications of Exosomes, Science, New York, N.Y., 2020, p. 367, https://doi.org/10.1126/science.aau6977.
[14] C. Cui, H. Lin, Y. Shi, R. Pan, Hypoxic postconditioning attenuates apoptosis via inactivation of adenosine A receptor through NDRG3-Raf-ERK pathway, Biochem. Biophys. Res. Commun. 491 (2017) 277–284, https://doi.org/10.1016/j.bbrc.2017.07.112.
[15] Z. Liu, Y. Xu, Y. Wan, J. Gao, Y. Chu, J. Li, Exosomes from adipose-derived mesenchymal stem cells prevent cardiomyocyte apoptosis induced by oxidative stress, Cell death discovery 5 (2019) 79, https://doi.org/10.1038/s41420-019-0159-5.
[16] B. Bertrand, P. Francois, J. Magalon, C. Philandrianos, F. Sabatier, Comparison of endothelial differentiation capacities of human and rat adipose-derived stem cells, Plast. Reconstr. Surg. 140 (2017) 511e–513e, https://doi.org/10.1097/prs.0000000000003632.
[17] R. Lai, T. Chen, S. Lim, Mesenchymal stem cell exosome: a novel stem cell-based therapy for cardiovascular disease, Regen. Med. 6 (2011) 481–492, https://doi.org/10.2217/rme.11.35.
[18] A. Majmundar, W. Wong, M. Simon, Hypoxia-inducible factors and the response to hypoxic stress, Mol. Cell 40 (2010) 294–309, https://doi.org/10.1016/j.molcel.2010.09.022.
[19] F. Collino, J. Lopes, S. Corrêa, et al., Adipose-derived mesenchymal stromal cells under hypoxia: changes in extracellular vesicles secretion and improvement of renal recovery after ischemic injury, cellular physiology and biochemistry, international journal of experimental cellular physiology, biochemistry, and pharmacology 52 (2019) 1463–1483, https://doi.org/10.33594/000000102.
[20] W. Liu, L. Li, Y. Rong, et al., Hypoxic mesenchymal stem cell-derived exosomes promote bone fracture healing by the transfer of miR-126, Acta Biomater. 103 (2020) 196–212, https://doi.org/10.1016/j.actbio.2019.12.020.
[21] D. Zhang, F. Lv, G. Wang, Effects of HIF-1α on diabetic retinopathy angiogenesis and VEGF expression, Eur. Rev. Med. Pharmacol. Sci. 22 (2018) 5071–5076, https://doi.org/10.26355/eurrev_201808_15699.
[22] Y. Han, J. Ren, Y. Bai, X. Pei, Y. Han, Exosomes from hypoxia-treated human adipose-derived mesenchymal stem cells enhance angiogenesis through VEGF/VEGF-R, Int. J. Biochem. Cell Biol. 109 (2019) 59–68, https://doi.org/10.1016/j.biocel.2019.01.017.
[23] K. Han, A. Kim, M. Kim, D. Kim, H. Go, D. Kim, Enhancement of angiogenic effects by hypoxia-preconditioned human umbilical cord-derived mesenchymal stem cells in a mouse model of hindlimb ischemia, Cell Biol. Int. 40 (2016) 27–35, https://doi.org/10.1002/cbin.10519.
[24] M. Wu, G. Yiang, W. Liao, et al., Current mechanistic concepts in ischemia and reperfusion injury, cellular physiology and biochemistry, international journal of experimental cellular physiology, biochemistry, and pharmacology 46 (2018) 1650–1667, https://doi.org/10.1159/000489241.
[25] A. Jokuszies, A. Niederbichler, M. Meyer-Marcotty, L. Lahoda, K. Reimers, P. Vogt, Influence of transendothelial mechanisms on microcirculation: consequences for reperfusion injury after free flap transfer. Previous, current, and future aspects, J. Reconstr. Microsurg. 22 (2006) 513–518, https://doi.org/10.1055/s-2006-951316.
[26] H. Liu, M.Z. Zhang, Y.F. Liu, X.H. Dong, Y. Hao, Y.B. Wang, Necroptosis was found in a rat ischemia/reperfusion injury flap model, Chin. Med. J. 132 (2019) 42–50, https://doi.org/10.1097/CM9.0000000000000005.
[27] G. Mariño, M. Niso-Santano, E. Baehrecke, G. Kroemer, Self-consumption: the interplay of autophagy and apoptosis, Nat. Rev. Mol. Cell Biol. 15 (2014) 81–94, https://doi.org/10.1038/nrm3735.
[28] H. Shen, P. Codogno, Autophagic cell death: loch Ness monster or endangered species? Autophagy 7 (2011) 457–465, https://doi.org/10.4161/auto.7.5.14226.